

STUDY OF STRAIN STATE AND FORCE PARAMETERS IN A WIRE DURING DEFORMATION BY A NEW COMBINED TECHNOLOGY

Andrey Volokitin¹, Evgeniy Panin¹, Irina Volokitina¹, Elisey Khlopkov^{2,3}

¹Karaganda Industrial University, 101400, 30 Republic Ave.
Temirtau, Kazakhstan, irinka.vav@mail.ru (I.V.); dyusha.vav@mail.ru (A.V.);
cooper802@mail.ru (E.P.).

²Peter the Great St. Petersburg Polytechnic University
195251, 29 Polytechnicheskaya St., St. Petersburg, Russia, hlopkovelisey@mail.ru (E.P.).

³Ioffe Institute, 194021, 26 Polytechnicheskaya St., St. Petersburg, Russia

Received 16 February 2024

Accepted 07 May 2024

DOI: 10.59957/jctm.v60.i2.2025.16

ABSTRACT

In this article, the influence of a new copper wire processing technology on the equivalent strain change was investigated. This technology consists in the wire deforming in a rotating equal-channel step matrix and subsequent drawing. The matrix rotates around the axis of the wire and thereby creates tension due to equal-channel angular broaching and twisting in the matrix. Deformation modelling was carried out at ambient temperature. To assess the effect of the twisting degree on the strain distribution, the rotation speed of the matrix was changed within 6, 18 and 30 rpm. The distance between the two deforming tools was also changed in the range of 100, 200 and 300 mm. The simulation results showed that an increase in the distance between the tools and the rotation speed of the matrix leads to an increase in the twisting angle and the total accumulated strain.

Keywords: wire, copper, drawing, twisting, modelling, equivalent strain, force.

INTRODUCTION

The purpose of any production is to implement a technological process in which multiple transformations of the source material into the finished product take place. In modern conditions, the consumer imposes a whole range of sometimes unique requirements on the wire, the achievement of which necessitated the creation of many varieties of the drawing process, the introduction of new technological solutions and equipment [1 - 3].

Nanostructuring processes make it possible to significantly modify the properties of alloys without changing their chemical composition and are one of the most progressive ways to improve the complex of mechanical properties of structural materials [4 - 7]. However, achieving a unique combination of particularly high strength and at the same time sufficient plasticity of ultrafine-grained materials requires the development of original methods for their production.

Currently, severe plastic deformation (SPD) processes are widely used to form an ultrafine-grained structure [8 - 12]. This applies to methods such as equal-channel angular pressing (ECAP) [13, 14], high-pressure torsion (HPT) [15, 16], all-round forging and others. In these methods, a distinctive feature is the accumulation of a significant degree of strain in the workpiece below the recrystallization temperature [17 - 19]. HPT is an effective method of strain accumulation, since in just 0.5 - 1 turn, even near the central region of the disk, a significant degree of strain is achieved $\varepsilon = 17 - 18$ [20]. To achieve the same degree of strain using ECAP, a significant number of passes are required, approximately 16, and during stretching, rolling and drawing, it is necessary to lengthen the sample ten million times. However, on an industrial scale, it is almost impossible to obtain long objects such as rods and wire using SPD methods.

Scientists from many countries are busy solving the issue of using SPD methods in drawing [21 - 23].

It was shown by Muszka et al. that the most efficient grain refinement occurs due to bending of the wire during drawing, which can be achieved, for example, by changing the location of the drawing tools relative to the axis of drawing [24]. The main disadvantages of such a scheme are the low drawing speed (0.05 m s^{-1}), the difficulty of filling the wire with each drawing and the complex system of the node with the lugs, the breakdown of which in industrial production can significantly reduce its productivity.

During the study, it was found that the combination of various processes allows for continuous deformation without the formation of a press residue in the matrix. One of these combined technologies is a technology that combines ECAP and traditional drawing (ECAP-drawing) [25]. The deformation technology being developed in this article represents a further development of the combined “ECAP-drawing” process. Since the use of rotating monolithic drawing tools and methods of rotating the front and rear ends of the wire do not allow a wire with an UFG structure, to obtain such a structure, it is necessary to set intense torsion with the tool, creating a helicoidal metal flow in the deformation zone. Therefore, in this developed technology, the key feature is the rotating ECA matrix. Due to this, in addition to deformation at the stages of ECAP and drawing, the workpiece receives a certain increase in strain due to twisting in the gap between two deforming tools.

The practical significance of this work lies in the possibility of introducing improved technology into existing drawing mills by adding a single node, without significant changes in the mill design or in the deformation technology. To determine the technological and geometric parameters of the process, a simulation of the developed technology in the Deform software package was carried out. The main mechanism of plastic deformation is shear. Therefore, the uniformity of the stress and strain states can be ensured if the directions and intensity of the shear coincide throughout the deformable volume. The strain state is the main characteristic of the processing of the material during metal forming. Analysing the level and uniformity of the distribution of the parameters of the strain state, the researcher has the opportunity to assess the effectiveness of the deformation scheme being developed. The equivalent strain, which includes all components of the main strains, is usually considered as the main parameter of the strain state. The

study of force parameters makes it possible to assess the loads acting on the deforming tool and identify the appropriate conditions for their occurrence.

EXPERIMENTAL

The strain rate v_1 applied to the front end of the workpiece and equal to 500 mm s^{-1} was taken as the initial parameter. In the fiber, the initial diameter of 7 mm is reduced to 6 mm. In accordance with the law of constancy of second volumes, the velocity v_{0-1} will be equal to 367 mm s^{-1} . The velocity v_0 applied to the rear end of the workpiece is 280 mm s^{-1} . At the same time, it was decided to vary the value of the rotation speed of the matrix to assess the effect of the level of twisting of the workpiece on the distribution of strain parameters. The following values of rotation speed of the matrix were set: 6, 18, 30 rpm. A geometric parameter such as the distance between two deforming tools was also varied. This variation was designed to evaluate the distribution of the twisting intensity in the interval between tools with unchanged kinematic parameters. The following values of the distance between the matrix and the fiber were set: 100, 200, 300 mm.

RESULTS AND DISCUSSION

To analyse the strain state, it is necessary to determine in advance the stages of the deformation process. In our case, the workpiece, passing through the channels of the ECA matrix, receives two levels of strain - due to shear at the joints of the channels and due to twisting from rotation of the matrix. After the ECAP stage, the workpiece enters the drawing tool, where the drawing stage takes place. For a discrete study of each stage, it is advisable to choose those stages at which it is possible to evaluate each stage separately. It was decided to investigate the strain state at the following stages:

- 1) workpiece passes $2/3$ of the distance between matrix and drawing tool. At this stage, it is possible to discretely assess the effect of ECAP with torsion and drawing (zones L01 and L02 in Fig. 1a, respectively);
- 2) workpiece with a deformed zone after ECAP with torsion partially exits the drawing tool. At this stage, it is possible to assess the overall impact of this combined scheme (zone L03 in Fig. 1b).

For each variant of the rotation speed, three cross

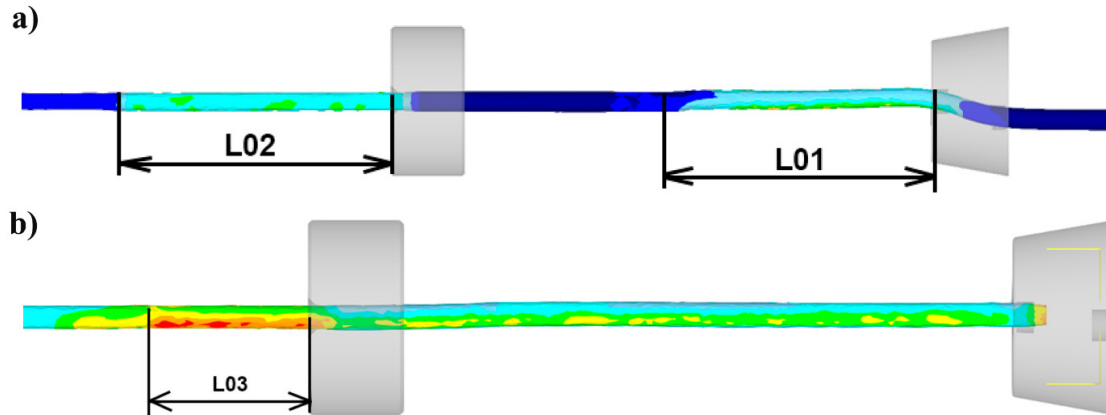


Fig. 1. Location of zones for the strain state study.

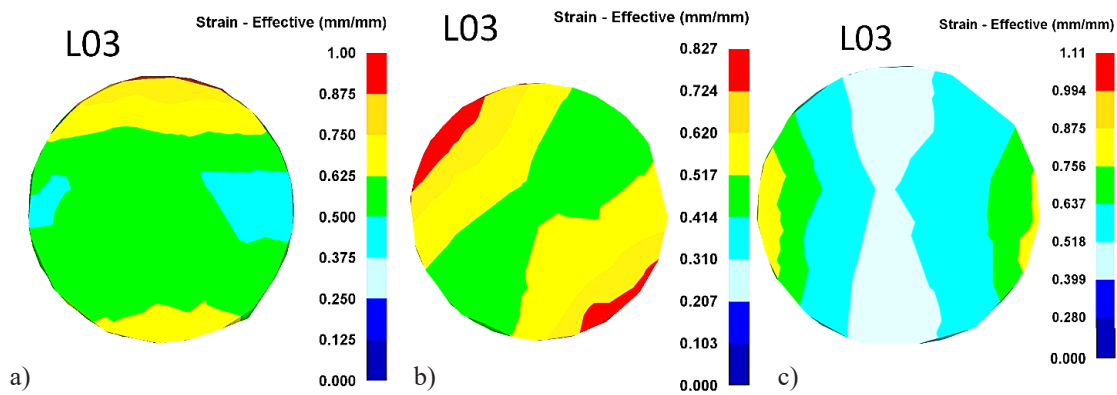


Fig. 2. Equivalent strain in the workpiece sections with a distance between the matrix and the drawing toll of 100 mm at different rotation speeds of the matrix: (a) - 6 rpm, (b) - 18 rpm, (c) - 30 rpm.

sections were made in each of the three mentioned zones. At the same time, in the L02 zone, after a single drawing stage, a limiting value of the strain scale was set equal to 0.5. This was done because in the interval between the tools, the workpiece receives a constant strain from twisting, as well as an additional strain level from the ECAP. At the same time, at the stage of single drawing, the strain level from compression in the drawing tool remains constant, and the difference in values between all models in the L02 zone will be the difference only from the twisting effect, which in turn depends on the rotation speed and the length of the twisting zone.

When analysing several models with variable parameters, it is advisable to accept any model as the base model with which the rest of the models will be compared. In this study, the optimal choice of the basic model will be a model with a distance between the matrix and the fiber of 100 mm and a rotation speed of

the matrix of 6 rpm, since this model has the minimum values of both variable parameters, and all other models have increased values of any one parameter or both at once. As a result of a comparative analysis of all models with the basic one, it will be possible to determine the effect of increasing these parameters on the level and distribution of strain over the cross section both after both discrete stages of deformation and after their combined effects.

Fig. 2 shows patterns of equivalent strain distribution for models with a distance between the matrix and the fiber of 100 mm at different rotation speeds of the matrix. Comparing the strain distribution in the L01 zone at all rotation speeds of the matrix, it can be noted that in all cases the nature of the strain distribution after ECAP is the same (layered) - on the upper and lower parts of the section, the strain level is higher (approximately 0.5 - 0.6) due to direct metal contact with the matrix in

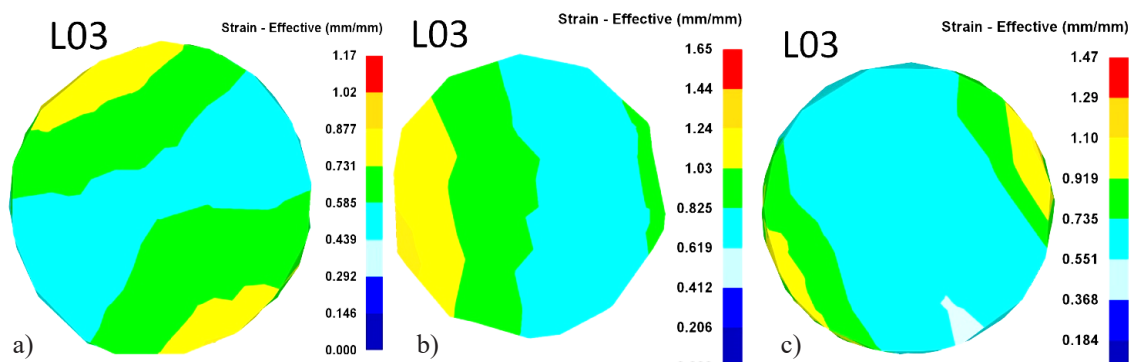


Fig. 3. Equivalent strain in the workpiece sections with a distance between the matrix and the drawing toll of 200 mm at different rotation speeds of the matrix: (a) - 6 rpm, (b) - 18 rpm, (c) - 30 rpm.

the zones of the junction of channels. The central zone has a lower strain level (approximately 0.25 - 0.3). It is also possible to note here the influence of the torsion stage of the matrix - due to the rotation of the tool, the usual horizontal distribution of strain fields receives a certain inclination angle, which increases with increasing rotation speed.

Comparing the strain distribution in the L02 zone at all rotation speeds of the matrix, it is possible to note the influence of the torsion stage in the matrix on the level and nature of the strain distribution over the cross section. With an increase in the rotation speed of the matrix after passing the gap between the two deforming tools, the surface layers receive an increased strain level. At the same time, the absolute increase in strain due to the torsion stage is relatively small (from 0.35 at minimum rotation speed to 0.45 at maximum speed).

Analysing the resulting strain level in the L03 zone, we can note a similar layered nature of the strain distribution with the L01 zone. This effect is manifested since initially in this area the strain distribution is formed in the L01 zone; after passing the drawing, the workpiece receives an increase in strain characteristic of the L02 zone, which is more homogeneous. In general, the action of the torsion stage is also observed here - with an increase in the rotation speed of the matrix, a more intense twisting of the workpiece occurs, at a speed of 30 rpm, a 90° rotation occurs, i.e. initially, the horizontal layers become vertical. The strain level on the upper and lower parts of the section reaches approximately 0.75 - 0.85. The central zone has a strain level of about 0.5 - 0.6.

Since a similar change in equivalent strain occurs in zones L01 and L02, only the L03 zone will be

considered for the following models. Fig. 3 shows patterns of equivalent strain distribution for models with a distance between the matrix and the fiber of 200 mm at different rotational speeds of the matrix. In the zone, at all speeds of rotation of the matrix, the character of the strain distribution after ECAP remains layered - on the upper and lower parts of the section, the strain level is about 0.5 - 0.6, and the central zone has a strain level of about 0.25 - 0.3. At the same time, an increased effect of matrix torsion can be noted here - due to an increase in the length of the gap between the tools, the twisting angle increases in all three models.

In the L03 zone, where the final level of strain is formed, it can be noted that an increase in the length of the gap between two deforming tools leads to a significant increase in the twisting. So, a 90° rotation occurs already at a speed of 18 rpm, and at a rotation speed of 30 rpm, the final twist angle is approximately 115 - 120°. The strain level on the upper and lower parts of the section reaches about 0.9-1.1. The central zone has a strain level of about 0.7 - 0.75.

Fig. 4 shows patterns of equivalent strain distribution for models with a distance between the matrix and the fiber of 300 mm at different rotational speeds of the matrix.

Due to the even greater distance between the fiber and the matrix, the twisting effect is more clearly manifested here. In the L03 zone, an increase in the gap between the deforming tools leads to an increase in the twisting angle. So, at a speed of 18 rpm, a rotation of 100° occurs, and at a rotation speed of 30 rpm, the final twist angle is approximately 135°. The strain level on the upper and lower parts of the section reaches about 0.95 - 1.15. The central zone has a strain level of about 0.7 - 0.8.

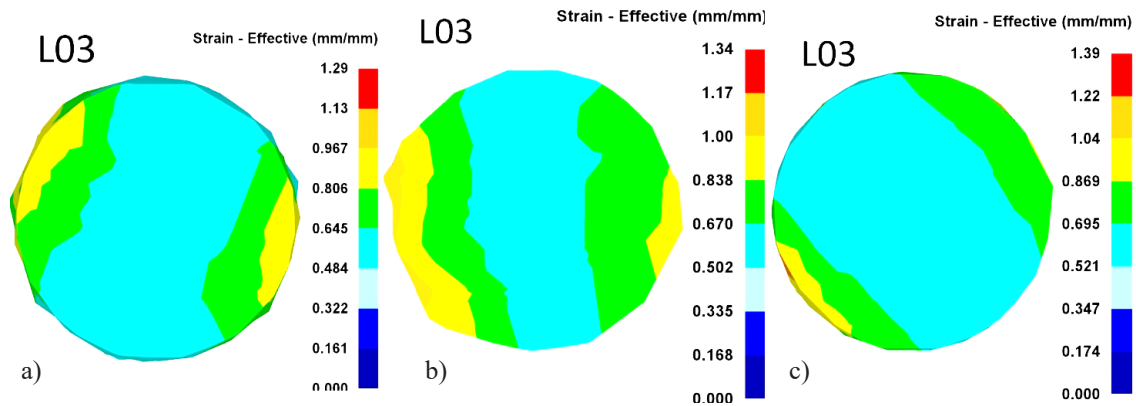


Fig. 4. Equivalent strain in the workpiece sections with a distance between the matrix and the drawing toll of 300 mm at different rotation speeds of the matrix: (a) - 6 rpm, (b) - 18 rpm, (c) - 30 rpm.

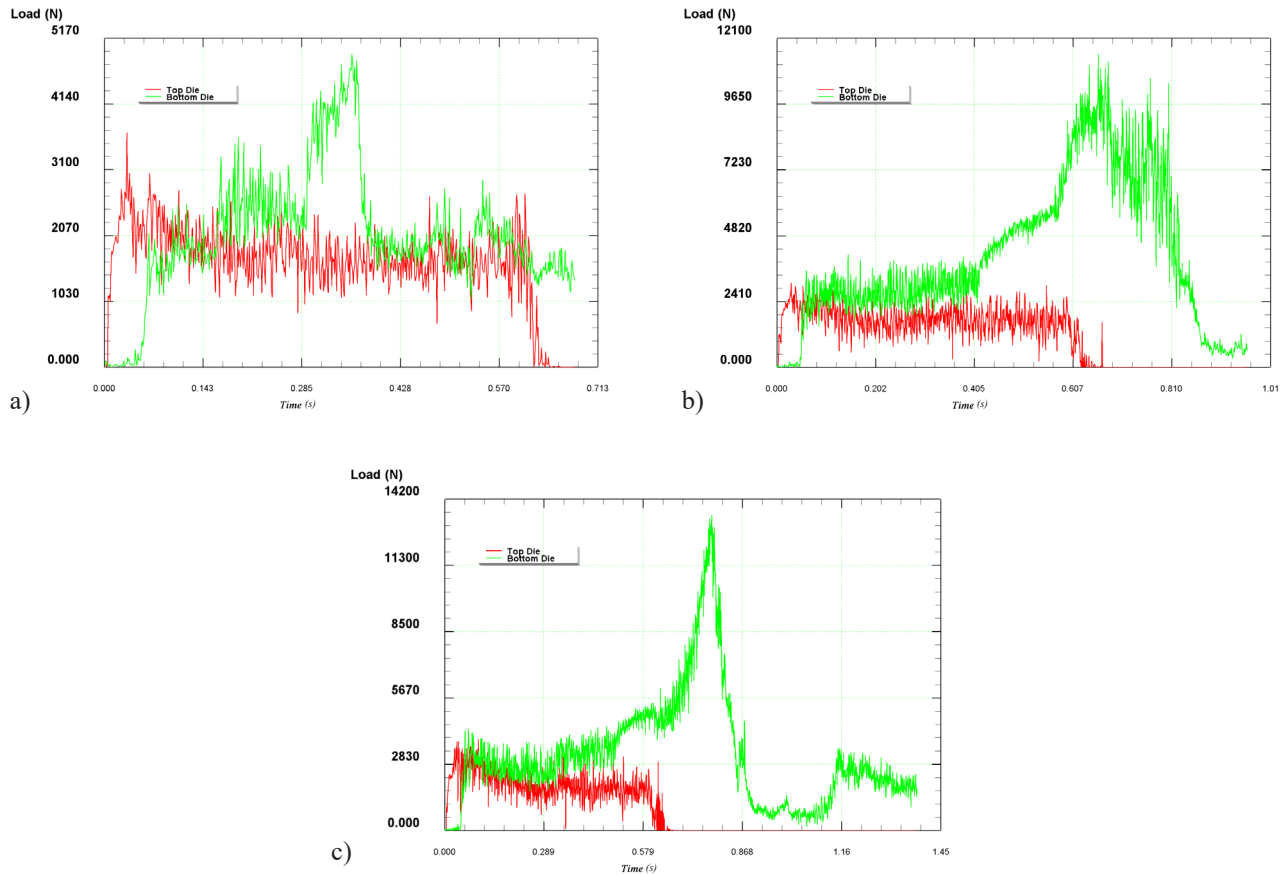


Fig. 5. Force graphs at a matrix rotation speed of 6 rpm with different distances between the matrix and the drawing tool: (a) - 100 mm; (b) - 200 mm; (c) - 300 mm

After studying the strain state, an important aspect of the investigation of any deformation technology is the force analysis, since this parameter is also critically important for assessing the durability of deforming equipment. Since the force graphs for all models will represent sequential curves for the ECA matrix and

the drawing tool, it was decided to swap the control parameters, i.e. consider groups of models depending on the matrix rotation speed, and within one group - on the gap size between tools. Fig. 5 shows the force graphs at a matrix rotation speed of 6 rpm with different distances between the matrix and the drawing tool.

Table 1. Peak forces in the drawing area, kN.

	6 rpm	18 rpm	30 rpm
100 mm	4.97	4.5	4.2
200 mm	11.6	9.4	8.2
300 mm	13.6	9.9	8.8

A comparison of the results revealed that the force on the ECA matrix in all models (Top Die in the models) is approximately the same and is equal to 2.2 - 2.4 kN. At the same time, the main differences are fixed at the drawing stage. Graphs of the drawing force (Bottom Die in the models) in this combined process in all models has a pronounced peak, which is characterized by the ingress into the drawing tool of a volume of metal previously deformed in the ECA matrix. After that, the process stabilizes and the level of force decreases. However, this peak has practical interest, since the possibility of overcoming it will allow the combined process to be carried out continuously and without damage to the deforming tool. For convenience, the peak values of the drawing forces were summarized in Table 1.

CONCLUSIONS

In this paper, a simulation of a new technology for processing copper wire is carried out. The technology consists in deforming the wire in a rotating equal-channel step matrix and subsequent traditional drawing. The analysis of the results showed that an increase in the rotation speed of the matrix and the distance between the matrix and the drawing tool leads to an increase in the accumulated strain and the twist angle of the cross section. At the same time, there is an increase in strain not only at the wire outlet from the drawing tool, but also in the gap between the deforming tools. The analysis of the resulting forces showed that the force level on the ECA matrix is relatively small, while the force on the drawing tool significantly depends on the matrix rotation speed and the length of the gap between tools. The maximum force occurs with a gap length of 300 mm and a low rotation speed, while increasing the rotation speed allows for a given gap length to significantly reduce the deformation force.

Acknowledgments

This research has been/was/is funded by the Science Committee of the Ministry of Science and Higher Education of the Republic of Kazakhstan (Grant No. AP19676903).

Authors' contributions: *Conceptualization, I.V., A.V.: methodology, I.V., E.P.: investigation, I.V., A.V.: data curation, E.P.: writing - original draft preparation, E.P., A.V.: writing-review and editing, I.V., E.P.*

REFERENCES

1. I. Volokitina, B. Sapargaliyeva, A. Agabekova, A. Volokitin, S. Syrlybekkyzy, A. Kolesnikov, G. Ulyeva, A. Yerzhanov, P. Kozlov, Study of changes in microstructure and metal interface Cu/Al during bimetallic construction wire straining, *Case Studies in Construction Materials*, 18, 2023, e02162.
2. D.P. Verma, Sh.A. Pandey, A. Bansal, Sh. Upadhyay, N.K. Mukhopadhyay, G.V.S. Sastry, R. Manna, Bulk Ultrafine-Grained Interstitial-Free Steel Processed by Equal-Channel Angular Pressing Followed by Flash Annealing, *J. Mater. Eng. Perform.*, 25, 2016, 5157-5166.
3. J. Li, Q. Mei, Y. Li, T. Wang, Production of Surface Layer with Gradient Microstructure and Microhardness on Copper by High Pressure Surface Rolling, *Metals*, 10, 2020, 73.
4. V.D. Sitdikov, I.V. Alexandrov, M.M. Ganiev, E.I. Fakhretdinova, G.I. Raab, Effect of temperature on the evolution of structure, crystallographic texture and the anisotropy of strength properties in the Ti grade 4 alloy during continuous ECAP, *Rev. Adv. Mater. Sci.*, 2015, 41-44.
5. I. Volokitina, A. Bychkov, A. Volokitin, A. Kolesnikov,

- Natural Aging of Aluminum Alloy 2024 After Severe Plastic Deformation, *Metallography, Microstructure, and Analysis*, 12, 3, 2023, 564-566.
6. E.P. Orlova, G.G. Kurapov, I. Volokitina, A. Turdaliev, Plasticity as a physical-chemical process of deformation of crystalline solids. *J. Chem. Technol. Metall.*, 51, 4, 2016, 451-457.
 7. H. Dyja, L. Lesik, A. Milenin, S. Mróz, Theoretical and experimental analysis of stress and temperature distributions during the process of rolling bimetallic rods, *J. Mater. Process. Technol.*, 2002, 125-126, 731-735.
 8. E.I. Fakhretdinova, G.I. Raab, R.Z. Valiev, Modeling of Metal Flow during Processing by Multi-ECAP-Conform, *Advanced Engineering, Materials*, 17, 12, 2015, 1723-1727.
 9. S.V. Dobatkin, T.C. Lowe, R.Z. Valiev, Investigations and Applications of Severe Plastic Deformation, NATO Science Series, Kluwer Academic Publishers, 2000, 13-22.
 10. A.V. Volokitin, I.E. Volokitina, E.A. Panin, Martensitic Transformation in AISI-316 Austenitic Steel During Thermomechanical Processing, *Metallography, Microstructure, and Analysis*, 11, 4, 2022, 673-675.
 11. P. Eslami, A. Karimi Taheri, An investigation on diffusion bonding of aluminum to copper using equal channel angular extrusion process, *Materials Letters*, 65, 2011, 1862-1864.
 12. S.S. Kazemi, M. Homayounfard, M. Ganjani, N. Soltani, Numerical and Experimental Analysis of Damage Evolution and Martensitic Transformation in AISI 304 Austenitic Stainless Steel at Cryogenic Temperature, *Progress in Materials Science*, 53, 2019, 893-979.
 13. I. Volokitina, Effect of preliminary heat treatment on deformation of brass by the method of ECAP, *Metal Science and Heat Treatment*, 63, 3-4, 2021, 163-167.
 14. S. Lezhnev, I. Volokitina, T. Koinov, Research of influence equal channel angular pressing on the microstructure of copper, *J. Chem. Technol. Metall.*, 49, 6, 2014, 621-630.
 15. I. Volokitina, A. Volokitin, D. Kuis, Deformation of Copper by High-Pressure Torsion, *J. Chem. Technol. Metall.*, 56, 2021, 643-647.
 16. A.V. Volokitin, I.E. Volokitina, E.A. Panin, Thermomechanical Treatment of Stainless-Steel Piston Rings, *Progress in Physics of Metals*, 23, 3, 2022, 411-437.
 17. G. Raab, R. Valiev, T. Lowe, Y. Zhu, Continuous processing of ultrafine grained Al by ECAP-Conform, *Materials Science and Engineering A*, 382, 2004, 30-34.
 18. I.E. Volokitina, A.V. Volokitin, E.A. Panin, Martensitic Transformations in Stainless Steels, *Progress in Physics of Metals*, 23, 4, 2022, 684-728.
 19. D.G. Emaleeva, G.C. Gun, M.V. Chukin, Increase of Mechanical Properties of Steel Wire by Formation of Submicrocrystalline Structure of Surface Coating in the Process of Equal Channel Angular Drawing, *Abstracts of International Symposium "Bulk Nanostructured Materials: from Fundamentals to Innovations"*. International Scientific Issue. Ufa, 2007, 134-135.
 20. A.P. Zhilyaev, T.G. Langdon, Using high-pressure torsion for metal processing: Fundamentals and applications. *Prog. Mater. Sci.*, 53, 2008, 893-979.
 21. Wei-Jen Cheng, Chaur-Jeng Wang, Study of microstructure and phase evolution of hot-dipped aluminide mild steel during high-temperature diffusion using electron backscatter diffraction, *Applied Surface Science*, 257, 2011, 4663-4668.
 22. A.V. Polyakov, I.P. Semenova, G.I. Raab, V. Sitdikov, R. Valiev, Peculiarities of ultrafine-grained structure formation in Ti Grade-4 using ECAP-Conform, *Advanced Materials Science*, 31, 1, 2012, 78-84.
 23. U. Chakkingal, A. Suriadi, P. Thomson, The development of microstructure and the influence of processing route during equal channel angular drawing of pure aluminum, *Mater. Sci. Eng. A*, 266, 1999, 241-249.
 24. K. Muszka, L. Madej, J. Majta, The effects of deformation and microstructure inhomogeneities in the Accumulative Angular Drawing (AAD), *Materials Science and Engineering: A*, 574, 2013, 68-74.
 25. I. Volokitina, Change in the microstructure and properties of steel-aluminum wire during "ECA-pressing - drawing" process, *J. Chem. Technol. Metall.*, 57, 2022, 631-636.

